

UMINにて構築した、症例登録システムを使用中である(<http://www.epoami2.com/>よりリンク)。

### (13) 症例登録代行入力サポート

トラブル等のために施設内で症例登録がスムーズにできない場合に遅延なく症例登録を行えるように、コールセンターにて症例登録を代行入力する体制を構築し、運用中である。

### (14) 登録症例進捗管理サポート

症例が登録される毎に、フォローアップ検査の日付をメールで案内するシステムを構築した。また、各参加施設で登録されている症例リストも併せて案内することにより、その施設でフォローアップすべき症例の検査予定を案内している。

### (15) 症例報告書データ入力システム

症例報告書データベースを構築し、運用を開始した。

### (16) コールセンター開設

24 時間 365 日対応をするため、コールセンターを開設し、一次受付および二次対応への連携を行う体制を構築し、運用中である。

### (17) 各施設での倫理委員会・先進医療 B 通過状況 (平成 26 年 3 月 3 日現在)

EPO-AMI-II 試験 倫理委員会・先進医療 B 通過状況				
	施設名	倫理 委員会 通過	先進 医療 B 申請	先進 医療 B 通過
1	新潟大学医歯学 総合病院	○	○	○
2	立川総合病院	○	○	○
3	獨協医科大学 病院	○	○	○

4	大阪大学医学部 附属病院	○	○	○
5	大阪警察病院	○	○	○
6	関西労災病院	準備 中	準備 中	準備 中
7	大阪府立急性期・ 総合医療センター	○	○	○
8	大阪医療センター	○	○	○
9	大阪労災病院	○	○	○
10	岡山大学病院	○	○	○
11	昭和大学 藤が丘病院	○	○	○
12	関東労災病院	○	○	○
13	榊原記念病院	○	○	○
14	小倉記念病院	○	○	○
15	国立循環器病 研究センター病院	○	○	○
16	大阪府済生会 千里病院	○	○	○
17	昭和大学病院	○	○	○
18	日本医科大学 付属病院	○	○	○
19	聖マリアンナ 医科大学	○	○	○
20	藤沢市民病院	再審 予定	準備 中	準備 中
21	湘南鎌倉総合病院	○	○	○
22	野崎徳洲会病院	○	○	○
23	東大阪市立 総合病院	○	○	○
24	千葉西総合病院	○	○	○
25	日本医科大学武蔵 小杉病院	○	準備 中	準備 中
26	千葉救急医療セン ター	○	○	○
27	江戸川病院	○	○	○

図 5

### (18) 症例登録

平成 26 年 2 月 14 日現在、127 症例登録されている。

### (19) デザイン論文の発表

本研究のデザイン論文を投稿し、アクセプトされた (*Cardiovasc Drugs Ther.* 26(5):409-16. 2012)。

### (20) 重篤な有害事象の報告

共同研究施設において、重篤な有害事象が発生した。独立効果安全性評価委員会による審議の結果、本研究との因果関係は否定できると判断され、研究代表者へ試験継続が勧告されたため、研究代表者が試験継続を決定した。本有害事象については、適切に、大阪大学医学部附属病院倫理委員会への詰問、先進医療制度および高度医療評価制度(先進医療 B)への報告を行っている。また、試験終了時には薬剤提供を受けている企業への報告を行う予定である。

### (21) 監査の実施

大阪大学医学部附属病院にて、本研究を適切に実施しているかについて、平成 25 年 3 月 21 日に外部独立機関による監査が実施された。

## D. まとめ

当初の計画に基づき、平成 23 年度中に参加施設倫理委員会申請と並行して高度医療評価制度申請を進めた。しかし、高度医療評価会議(現先進医療会議、平成 23 年 1 月、3 月開催)で、保険医療の観点から、対象、試験デザインについて変更の必要を指摘されたため、試験計画書の変更を行い、最終的に、平成 23 年 8 月厚生労働大臣告示で正式承認された。試験計画変更のため、各施設での倫理委員会の修正・再提出、また、登録症例数の増加に伴う共同研究施設の変更が必要となった。さらに、東北地方太平洋沖地震のため、中外製薬の試験薬作製工場が大きな影響を受け、

プラセボを含む試験薬製造に遅れが生じた。この間、高度医療評価制度が共同研究施設事務職員に十分に浸透していないこと、臨床研究に関する倫理指針を徹底したこと、本研究が医師自主臨床試験でありながら各施設薬剤部での薬剤管理体制確立など前例のない取り組みがおこなわれたため、通常より申請書類作成に時間を要している。しかし、平成 23 年 12 月 15 日から、大阪大学医学部附属病院を含む 20 施設で登録が開始された。今後、先進医療 B の実施施設として順次追加し、合計 27 施設で試験開始を目指した。

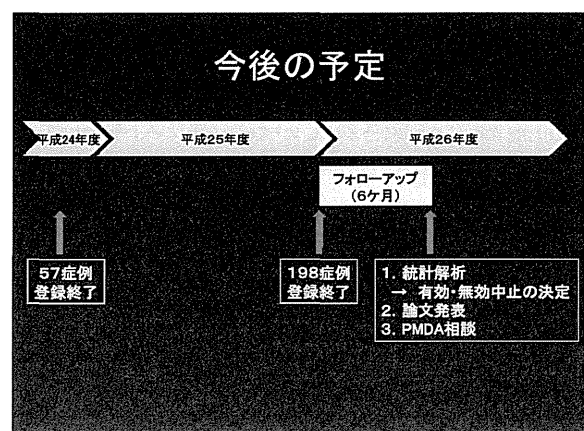


図 6

本研究を推進する中で、多施設臨床研究であるがゆえの問題点も明らかになってきた。それは、全参加施設における RI 撮像条件の統一を徹底するには多くの時間と労力を要すること、薬剤部・CRC の対応が勤務時間帯のみに限られるために緊急の症例登録に対応する体制が整っていない場合が多いことなどである。本研究を推進するなかで経験したことを生かし、今後、共同研究施設とも緊密に連絡を取り合い、患者登録を迅速に行っていく。

## EPO-AMI-IIの特長

1. 再灌流時薬物補充による新規心筋梗塞治療法の開発をめざすトランスレーショナル試験である
2. 二重盲検プラセボ対照多施設共同臨床研究であり“質の高いエビデンス”の世界発信が可能である
3. 先進医療Bを用いることにより、薬事申請をめざした臨床研究である
4. 日本の中核病院に対して、＜先進医療B＞、＜臨床研究に関する倫理指針＞の周知に貢献する
5. 日本循環器学会からの支援がある
6. 平成26年度中に成果を出す
7. インターネット、市民公開講座による国民への周知

図 7

## E. 健康危険情報

共同研究施設において、重篤な有害事象が発生した。独立効果安全性評価委員会による審議の結果、本研究との因果関係は否定できると判断され、研究代表者へ試験継続が勧告されたため、研究代表者が試験継続を決定した。本有害事象については、適切に、大阪大学医学部附属病院倫理委員会への詰問、先進医療制度および高度医療評価制度(先進医療 B)への報告、薬剤提供を受けている企業への報告を行っている。

## F. 研究発表

### 1. 論文発表

- 1) Kioka H, Kato H, Fujikawa M, Tsukamoto O, Suzuki T, Imamura H, Nakano A, Higo S, Yamazaki S, Matsuzaki T, Takafuji K, Asanuma H, Asakura M, Minamino T, Shintani Y, Yoshida M, Noji H, Kitakaze M, Komuro I, Asano Y, Takashima S.: Evaluation of intramitochondrial ATP levels identifies G0/G1 switch gene 2 as a positive regulator of oxidative phosphorylation. *Proc Natl Acad Sci U S A*. 2013
- 2) Takahashi A, Asakura M, Ito S, Min KD, Shindo K, Yan Y, Liao Y, Yamazaki S, Sanada S, Asano Y, Ishibashi-Ueda H,

Takashima S, Minamino T, Asanuma H, Mochizuki N, Kitakaze M.:

Dipeptidyl-peptidase IV inhibition improves pathophysiology of heart failure and increases survival rate in pressure-overloaded mice. *Am J Physiol Heart Circ Physiol*.

304(10):H1361-9. 2013

- 3) Takahama H, Shigematsu H, Asai T, Matsuzaki T, Sanada S, Fu HY, Okuda K, Yamato M, Asanuma H, Asano Y, Asakura M, Oku N, Komuro I, Kitakaze M, Minamino T.: Liposomal amiodarone augments anti-arrhythmic effects and reduces hemodynamic adverse effects in an ischemia/reperfusion rat model. *Cardiovasc Drugs Ther*.

27(2):125-32. 2013

- 4) Yoshida A, Asakura M, Asanuma H, Ishii A, Hasegawa T, Minamino T, Takashima S, Kanzaki H, Washio T, Kitakaze M.:. Derivation of a mathematical expression for predicting the time to cardiac events in patients with heart failure: a retrospective clinical study. *Hypertens Res*. 36(5):450-6. 2013

### 2. 学会発表

- 1) 南野哲男. 教育講演＜トランスレーショナルリサーチ実践による新しい心筋梗塞治療法の開発＞、第 61 回日本心臓病学会学術集会(2013 年 9 月:熊本)
- 2) 荒木 亮, 肥後修一郎, 南野哲男. <心筋梗塞患者に対するエリスロポエチン投与による心機能改善効果に関する研究 (EPO-AMI-II)>、第 116 回日本循環器学会近畿地方会(2013 年 11 月:大阪)

3) 肥後修一郎、南野哲男、鳥羽 健、小澤拓也、  
相澤義房、小室一成。

Erythropoietin-administration for the  
Treatment of Acute Myocardial  
Infarction (EPO-AMI-II Study) A Bridge  
from Bench to Clinical Practice  
第 21 回日本血管生物医学会学術集会  
(2013 年 9 月:大阪)

G. 知的財産権の出願・登録状況  
なし

# III. 研究成果の刊行に関する 一覧表

雑誌

発表者氏名	論文タイトル	発表誌名	巻号	ページ	出版日
Morita H, <u>Komuro I.</u>	A novel channelopathy in pulmonary arterial hypertension.	<i>N Engl J Med.</i>	369(22)	2161-2	2013
Nishimura S, Manabe I, Takaki S, Nagasaki M, Otsu M, Yamashita H, Sugita J, Yoshimura K, Eto K, <u>Komuro I.</u> , Kadowaki T, Nagai R.	Adipose Natural Regulatory B Cells Negatively Control Adipose Tissue Inflammation.	<i>Cell Metab.</i>	S1550-4131 (13)00386-0	[Epub ahead of print]	2013
Tamaki S, Mano T, Sakata Y, Ohtani T, Takeda Y, Kamimura D, Omori Y, Tsukamoto Y, Ikeya Y, Kawai M, Kumanogoh A, Hagihara K, Ishii R, Higashimori M, Kaneko M, Hasuwa H, Miwa T, Yamamoto K, <u>Komuro I.</u>	Interleukin-16 promotes cardiac fibrosis and myocardial stiffening in heart failure with preserved ejection fraction.	<i>PLoS One.</i>	8(7)	e68893.	2013
Miwa K, Lee JK, Takagishi Y, Opthof T, Fu X, Hirabayashi M, Watabe K, Jimbo Y, Kodama I, <u>Komuro I.</u>	Axon guidance of sympathetic neurons to cardiomyocytes by glial cell line-derived neurotrophic factor (GDNF).	<i>PLoS One.</i>	8(7)	e65202.	2013
Matsuda T, Miyagawa S, Fukushima S, Kitagawa-Sakakida S, Akimaru H, Horii-Komatsu M, Kawamoto A, Saito A, Asahara T, <u>Sawa Y.</u>	Human Cardiac Stem Cells With Reduced Notch Signaling Show Enhanced Therapeutic Potential in a Rat Acute Infarction Model.	<i>Circ J.</i>		[Epub ahead of print]	2013

Kawamura M, Miyagawa S, Fukushima S, Saito A, Miki K, Ito E, Sougawa N, Kawamura T, Daimon T, Shimizu T, Okano T, Toda K, <u>Sawa Y.</u>	Enhanced survival of transplanted human induced pluripotent stem cell-derived cardiomyocytes by the combination of cell sheets with the pedicled omental flap technique in a porcine heart.	<i>Circulation.</i>	128(11 Suppl 1)	S87-94.	2013
Shudo Y, Cohen JE, Macarthur JW, Atluri P, Hsiao PF, Yang EC, Fairman AS, Trubelja A, Patel J, Miyagawa S, <u>Sawa Y</u> , Woo YJ.	Spatially oriented, temporally sequential smooth muscle cell-endothelial progenitor cell bi-level cell sheet neovascularizes ischemic myocardium.	<i>Circulation.</i>	128(11 Suppl 1)	S59-68.	2013
Imanishi Y, Miyagawa S, Fukushima S, Ishimaru K, Sougawa N, Saito A, Sakai Y, <u>Sawa Y.</u>	Sustained-release delivery of prostacyclin analogue enhances bone marrow-cell recruitment and yields functional benefits for acute myocardial infarction in mice.	<i>PLoS One.</i>	8(7)	e69302.	2013
Kioka H, Kato H, Fujikawa M, Tsukamoto O, Suzuki T, Imamura H, Nakano A, Higo S, Yamazaki S, Matsuzaki T, Takafuji K, Asanuma H, Asakura M, <u>Minamino T</u> , Shintani Y, Yoshida M, Noji H, Kitakaze M, <u>Komuro I</u> , Asano Y, Takashima S.	Evaluation of intramitochondrial ATP levels identifies G0/G1 switch gene 2 as a positive regulator of oxidative phosphorylation.	<i>Proc Natl Acad Sci USA.</i>		[Epub ahead of print]	2013

<p>Takahashi A, Asakura M, Ito S, Min KD, Shindo K, Yan Y, Liao Y, Yamazaki S, Sanada S, Asano Y, Ishibashi-Ueda H, Takashima S, <u>Minamino T</u>, Asanuma H, Mochizuki N, Kitakaze M.</p>	<p>Dipeptidyl-peptidase IV inhibition improves pathophysiology of heart failure and increases survival rate in pressure-overloaded mice.</p>	<p><i>Am J Physiol Heart Circ Physiol.</i></p>	<p>304(10)</p>	<p>H1361-9.</p>	<p>2013</p>
<p>Takahama H, Shigematsu H, Asai T, Matsuzaki T, Sanada S, Fu HY, Okuda K, Yamato M, Asanuma H, Asano Y, Asakura M, Oku N, <u>Komuro I</u>, Kitakaze M, <u>Minamino T</u>.</p>	<p>Liposomal amiodarone augments anti-arrhythmic effects and reduces hemodynamic adverse effects in an ischemia/reperfusion rat model.</p>	<p><i>Cardiovasc Drugs Ther.</i></p>	<p>27(2)</p>	<p>125-32.</p>	<p>2013</p>
<p>Yoshida A, Asakura M, Asanuma H, Ishii A, Hasegawa T, <u>Minamino T</u>, Takashima S, Kanzaki H, Washio T, Kitakaze M.</p>	<p>Derivation of a mathematical expression for predicting the time to cardiac events in patients with heart failure: a retrospective clinical study.</p>	<p><i>Hypertens Res.</i></p>	<p>36(5)</p>	<p>450-6.</p>	<p>2013</p>

## IV. 研究成果の刊行物・別刷

# Interleukin-16 Promotes Cardiac Fibrosis and Myocardial Stiffening in Heart Failure with Preserved Ejection Fraction

Shunsuke Tamaki<sup>1,2</sup>, Toshiaki Mano<sup>1,2\*</sup>, Yasushi Sakata<sup>1</sup>, Tomohito Ohtani<sup>1</sup>, Yasuharu Takeda<sup>1</sup>, Daisuke Kamimura<sup>2,3</sup>, Yosuke Omori<sup>1,2</sup>, Yasumasa Tsukamoto<sup>1,2</sup>, Yukitoshi Ikeya<sup>1,4</sup>, Mari Kawai<sup>5</sup>, Atsushi Kumanogoh<sup>5</sup>, Keisuke Hagihara<sup>6</sup>, Ryohei Ishii<sup>7</sup>, Mitsuru Higashimori<sup>7</sup>, Makoto Kaneko<sup>7</sup>, Hidetoshi Hasuwa<sup>2</sup>, Takeshi Miwa<sup>2</sup>, Kazuhiro Yamamoto<sup>8</sup>, Issei Komuro<sup>1</sup>

**1** Department of Cardiovascular Medicine, Osaka University Graduate School of Medicine, Suita, Japan, **2** Genome Information Research Center, Osaka University, Suita, Japan, **3** Department of Medical Science and Cardiorenal Medicine, Yokohama City University Graduate School of Medicine, Yokohama, Japan, **4** Division of Cardiology, Department of Internal Medicine, Nihon University School of Medicine, Tokyo, Japan, **5** Department of Respiratory Medicine, Allergy and Rheumatic Diseases, Osaka University Graduate School of Medicine, Suita, Japan, **6** Department of Kampo Medicine, Osaka University Graduate School of Medicine, Suita, Japan, **7** Department of Mechanical Engineering, Osaka University, Suita, Japan, **8** Department of Molecular Medicine and Therapeutics, Faculty of Medicine, Tottori University, Yonago, Japan

## Abstract

**Background:** Chronic heart failure (CHF) with preserved left ventricular (LV) ejection fraction (HFpEF) is observed in half of all patients with CHF and carries the same poor prognosis as CHF with reduced LV ejection fraction (HFrEF). In contrast to HFrEF, there is no established therapy for HFpEF. Chronic inflammation contributes to cardiac fibrosis, a crucial factor in HFpEF; however, inflammatory mechanisms and mediators involved in the development of HFpEF remain unclear. Therefore, we sought to identify novel inflammatory mediators involved in this process.

**Methods and Results:** An analysis by multiplex-bead array assay revealed that serum interleukin-16 (IL-16) levels were specifically elevated in patients with HFpEF compared with HFrEF and controls. This was confirmed by enzyme-linked immunosorbent assay in HFpEF patients and controls, and serum IL-16 levels showed a significant association with indices of LV diastolic dysfunction. Serum IL-16 levels were also elevated in a rat model of HFpEF and positively correlated with LV end-diastolic pressure, lung weight and LV myocardial stiffness constant. The cardiac expression of IL-16 was upregulated in the HFpEF rat model. Enhanced cardiac expression of IL-16 in transgenic mice induced cardiac fibrosis and LV myocardial stiffening accompanied by increased macrophage infiltration. Treatment with anti-IL-16 neutralizing antibody ameliorated cardiac fibrosis in the mouse model of angiotensin II-induced hypertension.

**Conclusion:** Our data indicate that IL-16 is a mediator of LV myocardial fibrosis and stiffening in HFpEF, and that the blockade of IL-16 could be a possible therapeutic option for HFpEF.

**Citation:** Tamaki S, Mano T, Sakata Y, Ohtani T, Takeda Y, et al. (2013) Interleukin-16 Promotes Cardiac Fibrosis and Myocardial Stiffening in Heart Failure with Preserved Ejection Fraction. PLoS ONE 8(7): e68893. doi:10.1371/journal.pone.0068893

**Editor:** Xiongwen Chen, Temple University, United States of America

**Received:** January 30, 2013; **Accepted:** June 1, 2013; **Published:** July 19, 2013

**Copyright:** © 2013 Tamaki et al. This is an open-access article distributed under the terms of the Creative Commons Attribution License, which permits unrestricted use, distribution, and reproduction in any medium, provided the original author and source are credited.

**Funding:** This work was supported in part by grants from the Japanese Society for the Promotion of Science (No. 23591042 and No. 21590893) (<http://www.jpsps.go.jp/j-grantsnaid/index.html>). The funders had no role in study design, data collection and analysis, decision to publish, or preparation of the manuscript. No additional external funding received for this study.

**Competing Interests:** The authors have declared that no competing interests exist.

\* E-mail: mano@medone.med.osaka-u.ac.jp

## Introduction

Despite the progress in pharmacologic therapies, chronic heart failure (CHF) remains a major public health problem [1]. Approximately half of all patients with CHF have a preserved left ventricular (LV) ejection fraction, commonly referred to as heart failure with preserved ejection fraction (HFpEF) [2,3]. Therapies with proven benefit in heart failure with reduced ejection fraction (HFrEF) have failed to improve outcomes in HFpEF patients [3,4], which strongly suggests a different pathophysiology between HFpEF and HFrEF and the need for identification of a specific therapeutic target for HFpEF.

The primary cause of HFpEF has been attributed to an abnormality in diastolic function of the left ventricle, although the involvement of other factors such as increased arterial stiffness, sodium retention or neurohormonal activation in the development of HFpEF has also been suggested [5]. LV diastolic function has been divided into active relaxation and LV passive stiffness, and an abnormal elevation in LV passive stiffness has been shown in HFpEF patients [5]. Using an animal model of HFpEF, we clarified that LV stiffening plays a crucial role in the transition from asymptomatic diastolic dysfunction to HFpEF, and that LV myocardial fibrosis is an important cause of LV stiffening [6,7].

Recent evidence has shown that activation of the immune system plays an important role in CHF. Immune activation caused by myocardial injury, bacterial translocation and peripheral tissue hypoxia is thought to result in the production of pro-inflammatory mediators including tumor necrosis factor- $\alpha$ , interleukin (IL)-1 $\beta$  and IL-6 from mononuclear cells or the myocardium itself. These mediators have been reported to worsen CHF through their detrimental effect on myocardial contractility, LV remodeling or endothelial function [8,9]. Increased circulating levels of cytokines or chemokines have been shown to be associated with the severity of clinical symptoms and increased mortality [10,11]. However, these have been reported mainly in HFrEF patients or experimental models of CHF. There have been a few studies showing the association between cardiac inflammation and cardiac fibrosis or diastolic dysfunction [12–14], but the role of the immune system and specific inflammatory mediators involved in the development of HFpEF is not clear. Chronic inflammatory reactions promote fibrotic tissue remodeling, which can affect all organ systems including the heart [15,16]. From our previous studies and other studies, cardiac inflammation seems to be associated with the fibrotic process in HFpEF [17,18].

In this study, we aimed to identify novel inflammatory mediators associated with the development of HFpEF. Our results suggested that IL-16, a cytokine which has been shown to be a key

mediator of several inflammatory, allergic, or infectious diseases [19–21], promotes myocardial fibrosis, leading to increased LV myocardial stiffness.

## Methods

The clinical study was approved by Osaka University Hospital Ethical Committee (Permit Number: 09056-2, 10081-3), and conducted in accordance with the Declaration of Helsinki. All participants gave written informed consent. The experimental study was approved by the institutional ethics committee of Osaka University Graduate School of Medicine (Permit Number: 23-014-0, 23-030-1, 23-062-0), and conformed to the Guide for the Care and Use of Laboratory Animals published by the United States National Institutes of Health.

## Study Patients

Blood samples and echocardiograms were obtained from patients in Osaka University Hospital with a history of hospital admission for heart failure. Heart failure was clinically diagnosed according to the criteria used in the Framingham Heart Study project [22]. Patients with LV ejection fraction >40% and those with  $\leq$  40% were defined as HFpEF and HFrEF, respectively [4]. All patients were required to be in the compensated state at the time of blood sampling and echocardiography. Patients were

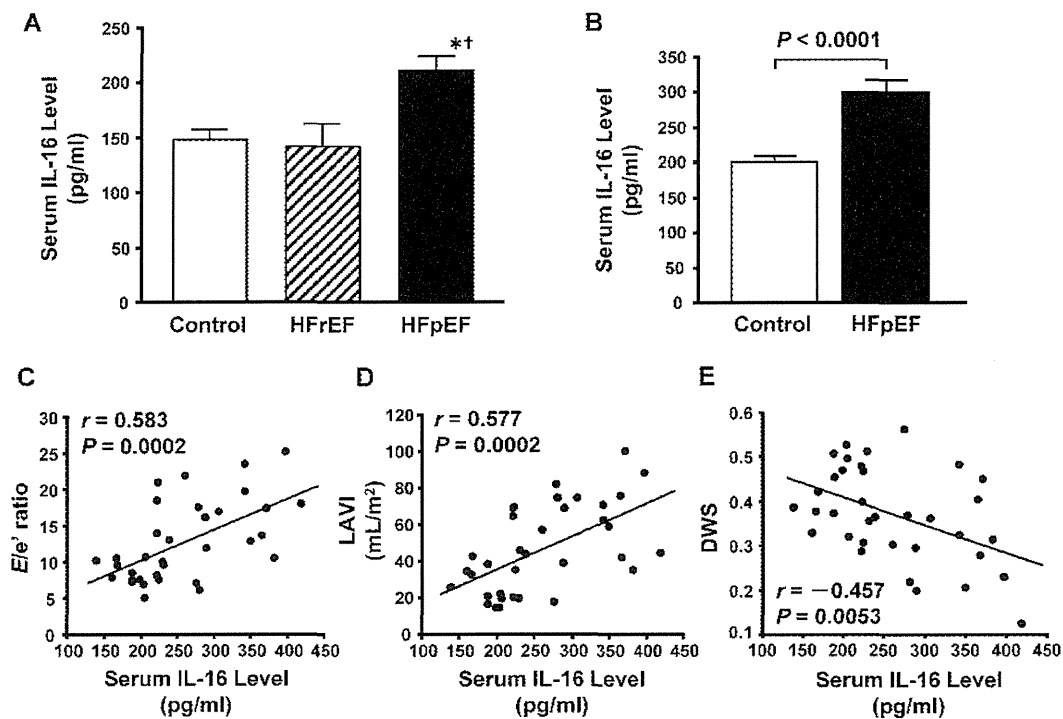


**Figure 1. Elevated serum interleukin-16 (IL-16) levels in patients with heart failure with preserved ejection fraction.** **A**, Serum IL-16 levels in controls and patients with heart failure with reduced (HFrEF) or preserved ejection fraction (HFpEF) measured by a multiplex-bead array assay. \* $P < 0.05$  vs. control group. † $P < 0.05$  vs. HFrEF group. **B**, Serum IL-16 levels in controls and patients with HFpEF measured by enzyme-linked immunosorbent assay. **C** through **E**, Correlations of serum IL-16 level and the ratio of early transmitral flow velocity to septal mitral annular early diastolic velocity ( $E/e'$  ratio) (**C**), left atrial volume index (LAVI) (**D**) and diastolic wall strain (DWS) (**E**) in controls and HFpEF patients combined. doi:10.1371/journal.pone.0068893.g001

**Table 1.** Clinical and study characteristics of controls and the patients with heart failure with reduced or preserved ejection fraction.

	Control (n=8)	HFrEF (n=9)	HFpEF (n=11)
Age, y	65+1	56+5	78+2*†
NYHA class I/II/III/IV	–	1/4/3/1	0/3/8/0
Body mass index, kg/m <sup>2</sup>	22.9+1.0	23.2+0.7	24.6+1.5
BNP, pg/ml	21+5	106+46	129+27
<b>Echocardiography</b>			
LV end-diastolic dimension, mm	43.4+1.3	64.7+1.5*	46.4+1.8†
EF, %	64.8+1.9	31.1+1.9*	67.9+2.3†

Data are mean + SEM. HFrEF and HFpEF indicate heart failure with reduced and preserved ejection fraction, respectively; NYHA, New York Heart Association; BNP, brain natriuretic peptide; LV, left ventricular; and EF, ejection fraction.

\*P<0.05 vs. control group.

†P<0.05 vs. HFrEF group.

doi:10.1371/journal.pone.0068893.t001

excluded from this study if they had acute coronary syndrome, ischemic cardiomyopathy, congenital heart disease, severe valvular disease, myocarditis, epicarditis, amyloidosis, significant renal dysfunction (serum creatinine level >2.0 mg/dl), active infectious diseases or cancer. Patients were also excluded if they had a history of bronchial asthma or any allergic, inflammatory or granulomatous disease, or were receiving systemic or topical corticosteroid therapy or any other immunomodulating medications. Medications were not withheld in the patients with HFpEF or HFrEF for ethical reasons. Healthy volunteers served as a control group. Venous blood was drawn from a superficial forearm vein following an overnight fast. Serum was obtained by allowing the blood sample to clot at room temperature for 1 hour followed by centrifugation.

#### Echocardiography in Human Subjects

Transthoracic echocardiography was performed according to standard techniques using a commercially available machine as previously described [23,24]. LV ejection fraction was calculated by Teichholz's formula or Simpson's rule. The LV mass index and relative wall thickness were calculated, early transmitral flow velocity (*E*) was measured by pulsed-wave Doppler, and the septal mitral annular early diastolic velocity (*e'*) was determined by spectral tissue Doppler imaging using standard methods as previously described [23]. Left atrial volume index (LAVI) was calculated in the apical 4-chamber view by the single-plane, area-length method [25]. Diastolic wall strain (DWS), a non-invasive index of LV passive stiffness, was calculated as follows:  $DWS = (PW_s - PW_d)/PW_s$ , where  $PW_s$  indicates posterior wall thickness at end-systole and  $PW_d$  indicates posterior wall thickness at end-diastole [23,26]. Systolic and diastolic blood pressure and heart rate were measured at the time of echocardiography.

#### Multiplex-bead Array Assay

Human serum samples were analyzed using Bio-Plex human cytokine 23-plex and 27-plex panel assays (Bio-Rad). The assay was performed according to the manufacturer's protocol. The resulting raw data were collected using the Bio-Plex 200 system (Bio-Rad) and analyzed using Bio-Plex Manager 5.0 software (Bio-Rad).

**Table 2.** Serum levels of analytes (excluding IL-16) that were significantly different among the controls and two patient groups.

	Control (n=8)	HFrEF (n=9)	HFpEF (n=11)
MIG	692.0+50.5	1525.4+533.1	5470.8+1594.6*†
SCF	106.4+6.0	131.7+17.3	206.2+21.4*†
Eotaxin	43.3+5.2	43.5+5.3	70.0+9.4*†
IP-10	413.5+60.8	564.1+68.9	853.1+111.0*

Data are mean + SEM. Values are in pg/ml. HFrEF and HFpEF indicate heart failure with reduced and preserved ejection fraction, respectively; MIG, monokine induced by interferon- $\gamma$ ; SCF, stem cell factor; and IP-10, interferon-inducible protein 10.

\*P<0.05 vs. control group.

†P<0.05 vs. HFrEF group.

doi:10.1371/journal.pone.0068893.t002

#### HFpEF Rat Model

Male Dahl salt-sensitive rats (SLC Japan) were fed a high-salt (8% NaCl) diet (Oriental Yeast Co.) starting at 6 weeks of age and served as the hypertensive HFpEF model as previously described [6,7,17,23,27]. Male Dahl salt-sensitive rats fed 0.3% NaCl chow served as age-matched controls. The data were obtained around 21 weeks of age, when this HFpEF model shows signs of overt heart failure with increased LV filling pressure and pulmonary congestion, without any significant changes in LV dimensions or fractional shortening [6,7,17,23,27]. Systolic blood pressure was measured with a tail-cuff system (BP-98A, Softron).

#### Echocardiography, Hemodynamic Studies and Tissue Sampling in Rats

Rats were anesthetized with intraperitoneal ketamine and xylazine (80 and 10 mg/kg, respectively), transthoracic echocardiography was performed and M-mode echocardiograms were recorded using an echocardiographic machine equipped with a 12-MHz transducer (SONOS 5500, Philips Medical System), as previously described [27]. The adequacy of anesthesia was monitored by the stability of blood pressure, heart rate and lack of flexor responses to a paw-pinch. A 1.5-F, high-fidelity, manometer-tipped catheter (SPR-407, Millar Instruments) was introduced through the right carotid artery into the left ventricle to determine the LV end-diastolic pressure (LVEDP), the time constant of LV relaxation ( $\tau$ ), and the myocardial stiffness constant (MSC) as previously described [27]. Following the hemodynamic study and additional anesthesia, blood was collected from the *vena cava*, and rats were euthanized by removal of the heart. The heart and lungs were rapidly harvested and weighed.

#### Transgenic Mice

Mouse IL-16 cDNA was isolated by reverse transcriptase-polymerase chain reaction from mouse spleen total RNA and cloned into the plasmid containing the  $\alpha$ -myosin heavy chain ( $\alpha$ -MHC) promoter and a simian virus 40 polyadenylation site. The construct was linearized, gel purified and microinjected into the pronuclei of BDF1 (C57BL/6  $\times$  DBA/2) mouse zygotes. Transgenic (TG) mice were identified by PCR, with primers specific for the  $\alpha$ -MHC promoter and IL-16 cDNA. IL-16 TG mice were crossed with C57BL/6 mice (SLC Japan), and the male F2 mice were used in the present study. The littermates of TG mice were used as non-transgenic (Non-TG) mice. All mice were analyzed at 20–22 weeks of age.

**Table 3.** Clinical and study characteristics of controls and the patients with heart failure with preserved ejection fraction.

	Control (n = 14)	HFpEF (n = 21)
Age, y	61±2	70±3
Male sex, n (%)	5 (36)	11 (52)
NYHA class I/II/III/IV	–	3/9/9/0
Height, m	1.58±0.02	1.59±0.02
Body weight, kg	55±2	62±3*
Body mass index, kg/m <sup>2</sup>	22.1±0.6	24.6±1.1
Systolic blood pressure, mmHg	124±4	124±4
Diastolic blood pressure, mmHg	75±2	66±3*
Heart rate, bpm	67±4	67±3
Hemoglobin, g/dL	13.8±0.3	12.5±0.4*
Creatinine, mg/dL	0.63±0.05	1.23±0.06*
eGFR, mL/min/1.73m <sup>2</sup>	86±3	44±4*
BNP, pg/ml	17±3	216±57*
<b>Echocardiography</b>		
LV end-diastolic dimension, mm	44.4±0.8	48.3±1.3*
LV end-systolic dimension, mm	27.9±0.9	32.2±1.3*
IVSd, mm	7.0±0.3	11.0±0.6*
PWd, mm	7.0±0.2	9.5±0.5*
LV mass index, g/m <sup>2</sup>	61.3±3.1	112.1±8.8*
RWT	0.32±0.01	0.40±0.02*
EF, %	67.3±1.6	61.4±2.3
E, m/s	0.64±0.05	0.82±0.06*
DcT, ms	191±15	208±13
e', cm/s	7.6±0.6	5.5±0.4*
E/e' ratio	8.7±0.6	15.5±1.2*
LAVI, mL/m <sup>2</sup>	24.7±2.8	61.3±4.1*
DWS	0.45±0.02	0.32±0.02*

Data are mean ± SEM. HFpEF indicates heart failure with preserved ejection fraction; NYHA, New York Heart Association; eGFR, estimated glomerular filtration rate; BNP, brain natriuretic peptide; LV, left ventricular; IVSd, interventricular wall thickness at end-diastole; PWd, LV posterior wall thickness at end-diastole; RWT, relative wall thickness; EF, ejection fraction; E, early transmitral flow velocity; DcT, deceleration time of early transmitral flow velocity; e', septal mitral annular early diastolic velocity; LAVI, left atrial volume index; and DWS, diastolic wall strain.  
\*P<0.05 vs. control group.  
doi:10.1371/journal.pone.0068893.t003

**A Mouse Model of Hypertension and IL-16 Neutralization**

ALZET osmotic minipumps (DURECT Corp.) were implanted subcutaneously in male C57BL/6 mice (SLC Japan) at 8–10 weeks of age for the administration of angiotensin II (Ang II) (1.2 mg/kg/day; A-9525, Sigma-Aldrich, Inc.) for 14 or 28 days. Osmotic minipumps containing saline were implanted in control mice. Mice were anesthetized with intraperitoneal ketamine and xylazine (100 and 10 mg/kg, respectively) to implant the osmotic minipumps. The adequacy of anesthesia was determined by the absence of a pedal reflex. To block the effect of IL-16, a group of Ang II-treated mice received an intraperitoneal injection of 200 µg anti-IL-16 neutralizing monoclonal antibody clone 14.1 (BD Biosciences) 3 times per week starting 1 day before and continuing until 14 or 28 days after the implantation of the osmotic minipumps, based on previous reports [28,29]. The other groups of Ang II-treated mice and the saline-infused control mice

**Table 4.** Hemodynamic, pathological and echocardiographic parameters of Dahl salt-sensitive rats.

	Control (n = 8)	HFpEF (n = 12)
Body weight, g	422±10	389±7*
Systolic blood pressure, mmHg	129±3	219±5*
Heart rate, bpm	393±12	452±9*
LV weight/body weight, mg/g	2.09±0.02	3.28±0.10*
Lung weight/body weight, mg/g	3.44±0.08	4.39±0.23*
<b>Echocardiography</b>		
LV end-diastolic dimension, mm	9.47±0.15	9.09±0.18
PWd, mm	1.10±0.02	1.73±0.04*
Fractional shortening, %	31±1	33±1
Midwall fractional shortening, %	19±1	19±1
<b>Catheterization</b>		
LV end-diastolic pressure, mmHg	1.8±0.4	7.3±1.2*
Tau, ms	16±1	28±3*
MSC	2.4±0.2	6.3±0.4*

Data are mean ± SEM. HFpEF indicates heart failure with preserved ejection fraction; LV, left ventricular; PWd, LV posterior wall thickness at end-diastole; Tau, time constant of LV relaxation; and MSC, myocardial stiffness constant.  
\*P<0.05 vs. control group.  
doi:10.1371/journal.pone.0068893.t004

received an intraperitoneal injection of phosphate buffered saline (PBS).

**Echocardiography and Tissue Sampling in Mice**

Transthoracic echocardiography was performed in conscious mice using the Vevo 770 Imaging System equipped with a 25-MHz linear probe (Visual Sonics). After echocardiography, mice were adequately anesthetized with intraperitoneal ketamine and xylazine (100 and 10 mg/kg, respectively) and euthanized by removal of the heart. An adequate anesthetic depth was determined by the absence of the pedal reflex. The heart and lungs were quickly harvested, and hearts were then promptly perfused through the aorta with ice-cold Ca<sup>2+</sup>-free Tyrode's solution containing 30 mM 2,3-butanedione monoxime (BDM). The left ventricle was sectioned perpendicularly to the longitudinal axis to obtain a transverse section at the mid-level of the heart with a 2–3 mm thickness, and this was used for the measurement of myocardial stiffness. LV samples for immunohistochemistry were embedded in Tissue Tek OCT compound (Sakura Finetechnical Co. Ltd.). The apical part of LV myocardium was snap-frozen in liquid nitrogen and stored for the measurement of mRNA and protein levels. The rest of the LV specimen was fixed with phosphate-buffered 10% formalin solution, embedded in paraffin, and 3 µm thick transverse cross-sections from the midventricular plane were stained with Sirius Red.

**Measurement of LV Myocardial Stiffness in Mice**

Skinned LV muscles from mice were prepared according to previously reported methods [30]. Transverse sections of the left ventricle were skinned in relaxing solution (5 mM MgATP, 40 mM BES, 1 mM Mg<sup>2+</sup>, 10 mM EGTA, 1 mM dithiothreitol, 15 mM phosphocreatine, 15 U/ml creatine phosphokinase, 10 mM BDM, 180 mM ionic strength [adjusted by K-propionate], pH 7.0) containing 1% Triton X-100 overnight. The specimens were then washed thoroughly with relaxing solution and stored in relaxing solution containing 50% glycerol. All

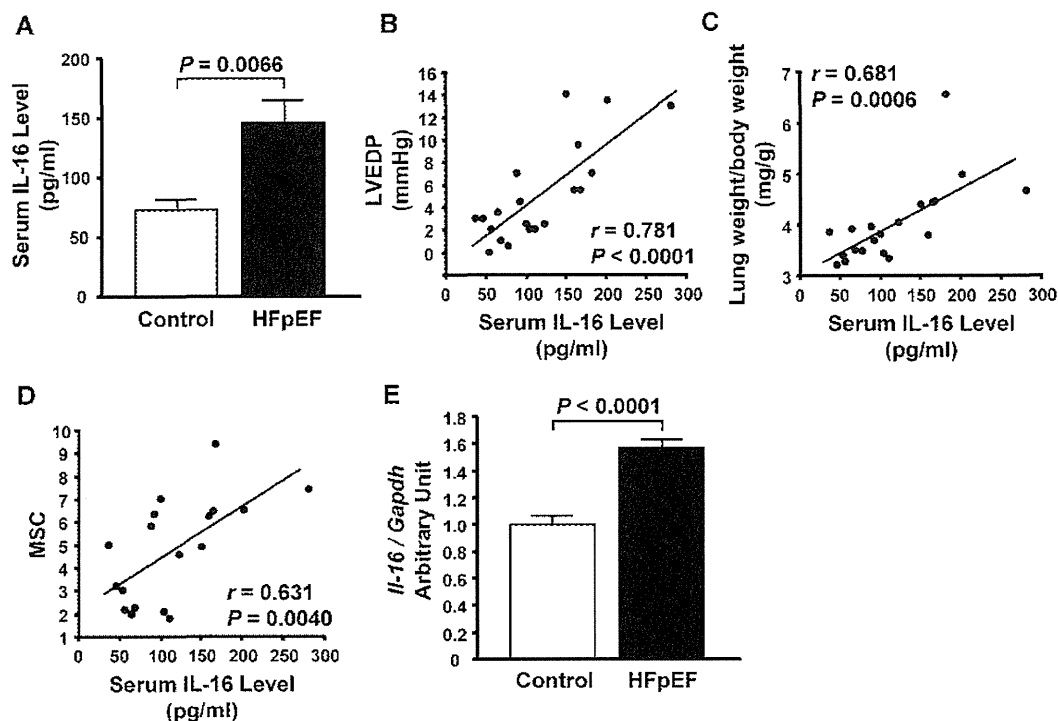


**Figure 2. Elevated serum interleukin-16 (IL-16) levels in rats with heart failure with preserved ejection fraction (HFpEF).** A, Serum IL-16 levels in control rats and the rats with HFpEF. B through D, Correlations of serum IL-16 level and left ventricular end-diastolic pressure (LVEDP) (B), lung weight to body weight ratio (lung weight/body weight) (C) and myocardial stiffness constant (MSC) (D) in control and HFpEF rats combined. E, mRNA level of IL-16 in the left ventricle of control and HFpEF rats. doi:10.1371/journal.pone.0068893.g002

solutions contained protease inhibitors (0.5 mM PMSF, 0.04 mM leupeptin and 0.01 mM E64).

We used a balloon-type sensing system to evaluate LV myocardial stiffness [31]. The skinned transverse section was placed around a latex balloon (Labo Support), while the pressure inside the balloon was monitored. The balloon was then dilated with the deformation information of the balloon and the specimen captured by a CCD camera. Young's modulus  $E_H$  was obtained from the internal pressure of the balloon and the strain of the transverse LV section based on a dual cylinder model.

#### Western Blot Analysis

Proteins were extracted from the left ventricle of the mice as previously described [32]. Proteins were separated on SDS-PAGE gels and transferred to PVDF membranes (Millipore). Membranes were probed with antibodies to IL-16 (1:200; MAB1727, R&D Systems), Collagen I (1:500; AB765P, Millipore), transforming growth factor-beta 1 (TGF- $\beta$ 1) (1:200; sc-146, Santa Cruz Biotechnology, Inc.) and connective tissue growth factor (CTGF) (1:5000; ab6992, Abcam). Blots were developed using enhanced chemiluminescence and expression levels were quantified using LAS-4000 and MultiGauge software (Fujifilm). The band density of the protein of interest was normalized to GAPDH expression (1:10000; sc-25778, Santa Cruz Biotechnology, Inc.).

#### Immunohistochemistry

Cryostat-frozen LV transverse cross-sections from the midventricular plane (8 $\mu$ m thick) were labeled with anti-IL-16 (1:100; sc-7902, Santa Cruz Biotechnology, Inc.), anti-F4/80 (1:100; MCA497, Serotec) and anti-TGF- $\beta$ 1 (1:50; sc-146-G, Santa Cruz Biotechnology, Inc.) antibodies. Fluorophore-conjugated secondary antibodies (Invitrogen) were applied, and stained samples were mounted with ProLong Gold antifade reagent with DAPI (Invitrogen). To evaluate macrophage infiltration, images of 12 random regions of the section were captured at  $\times$ 400 magnification using a fluorescence microscope (BZ-9000, Keyence), and F4/80-positive cells were counted and expressed as cells per square millimeter of myocardium as previously described [33]. Confocal images were obtained using a laser scanning microscope (TCS SP5, Leica).

#### Measurement of Myocardial Fibrosis

National Institutes of Health ImageJ software (Version 1.45) was used to measure the amount of myocardial fibrosis on sections stained by Sirius Red. In each section, 5 fields were randomly selected and the percent area of fibrosis was determined by the ratio of the Sirius Red-stained area to total myocardial area [34]. Fibrosis of the perivascular, epicardial and endocardial areas were excluded from the measurements [35].

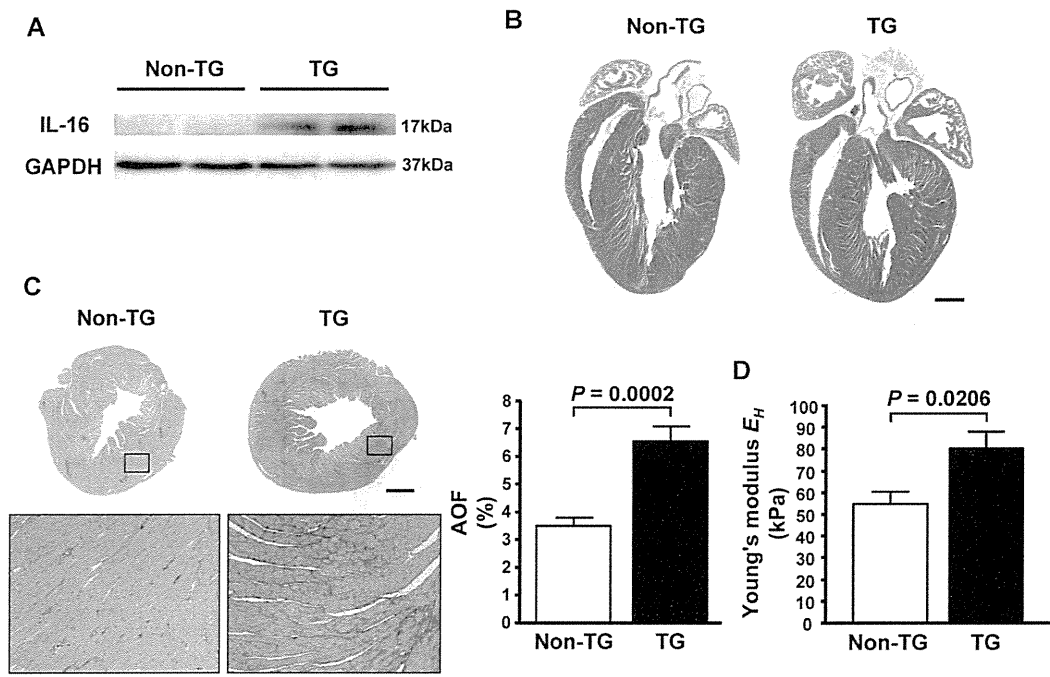


**Figure 3. Enhanced cardiac expression of interleukin-16 (IL-16) causes increased myocardial fibrosis and stiffness in mice.** **A**, Cardiac expression of IL-16 protein in non-transgenic (Non-TG) and transgenic (TG) mice. **B**, Four-chamber view of the hearts from Non-TG and TG mice stained with hematoxylin and eosin. Bar=1 mm. **C**, Representative photomicrograph of Sirius Red-stained heart sections and the percent area of fibrosis (AOF) of Non-TG and TG mice. Bar: Upper panel = 1 mm; Lower panel = 200  $\mu$ m. **D**, Young's modulus  $E_H$  in Non-TG and TG mice. doi:10.1371/journal.pone.0068893.g003

#### Cell Culture

Peritoneal cells were collected from male C57BL/6 mice (SLC Japan) at 6–8 weeks of age by peritoneal lavage with 10 ml of PBS after euthanasia by cervical dislocation. The cells were centrifuged, resuspended in DMEM supplemented with 10% FBS and incubated on a 12-well plate ( $2 \times 10^6$  cells/well). The cells were incubated to allow macrophages to adhere to the bottom of the plates. The plates were then washed gently with PBS to remove nonadherent cells, and the macrophages were incubated in serum-free medium containing murine recombinant IL-16 (Shenandoah Biotechnology Inc.) for 24 h. Supernatants were collected from the cell cultures.

#### Enzyme-linked Immunosorbent Assay

The concentration of IL-16 in human, rat and mouse serum samples was measured by commercially available enzyme-linked immunosorbent assay (ELISA) kits specific for human (R&D Systems), rat and mouse (Cusabio) IL-16, respectively. The concentration of TGF- $\beta$ 1 in the macrophage culture medium was determined using a commercially available ELISA kit for mouse TGF- $\beta$ 1 (R&D Systems).

#### Quantification of Gene Expression

Total RNA was isolated from the left ventricle, and the mRNA level was quantified by real-time quantitative polymerase chain reaction with the ABI PRISM 7900 HT Sequence Detection

System and Software (Applied Biosystems) as previously described [32]. Sequences of primers and probes and TaqMan gene expression assay IDs purchased from Applied Biosystems were as follows: rat IL-16: Rn01477714\_g1; rat GAPDH: Rn99999916\_s1; mouse Collagen I: Mm00801666\_g1; mouse TGF- $\beta$ 1: forward 5'-TGA CGT CAC TGG AGT TGT ACG G-3', reverse 5'-GGT TCA TGT CAT GGA TGG TGC-3', TaqMan probe 5'-TTC AGC GCT CAC TGC TCT TGT GAC AG-3'; mouse CTGF: forward 3'-AGC CGC CTC TGC ATG GTC A-3', reverse 5'-GCG ATT TTA GGT GTC CGG AT-3', TaqMan probe, 5'-CCT GCG AAG CTG ACC TGG AGG AAA-3'; mouse IL-16: Mm01317937\_g1; mouse F4/80: Mm00802529\_m1; mouse GAPDH: Mm99999915\_g1. All data were normalized to GAPDH expression.

#### Statistical Analysis

Data are presented as mean  $\pm$  SEM. Data were analyzed using statistical software (StatView version 5.0, SAS Institute Inc.). Differences between two groups for continuous and discrete variables were analyzed with an unpaired Student's *t*-test and Fisher's exact test, respectively. Differences among more than two groups were assessed by one-factor ANOVA followed by a Tukey-Kramer multiple comparison test. Correlations between variables were determined by Pearson's correlation coefficient. A *P* value <0.05 was considered statistically significant.

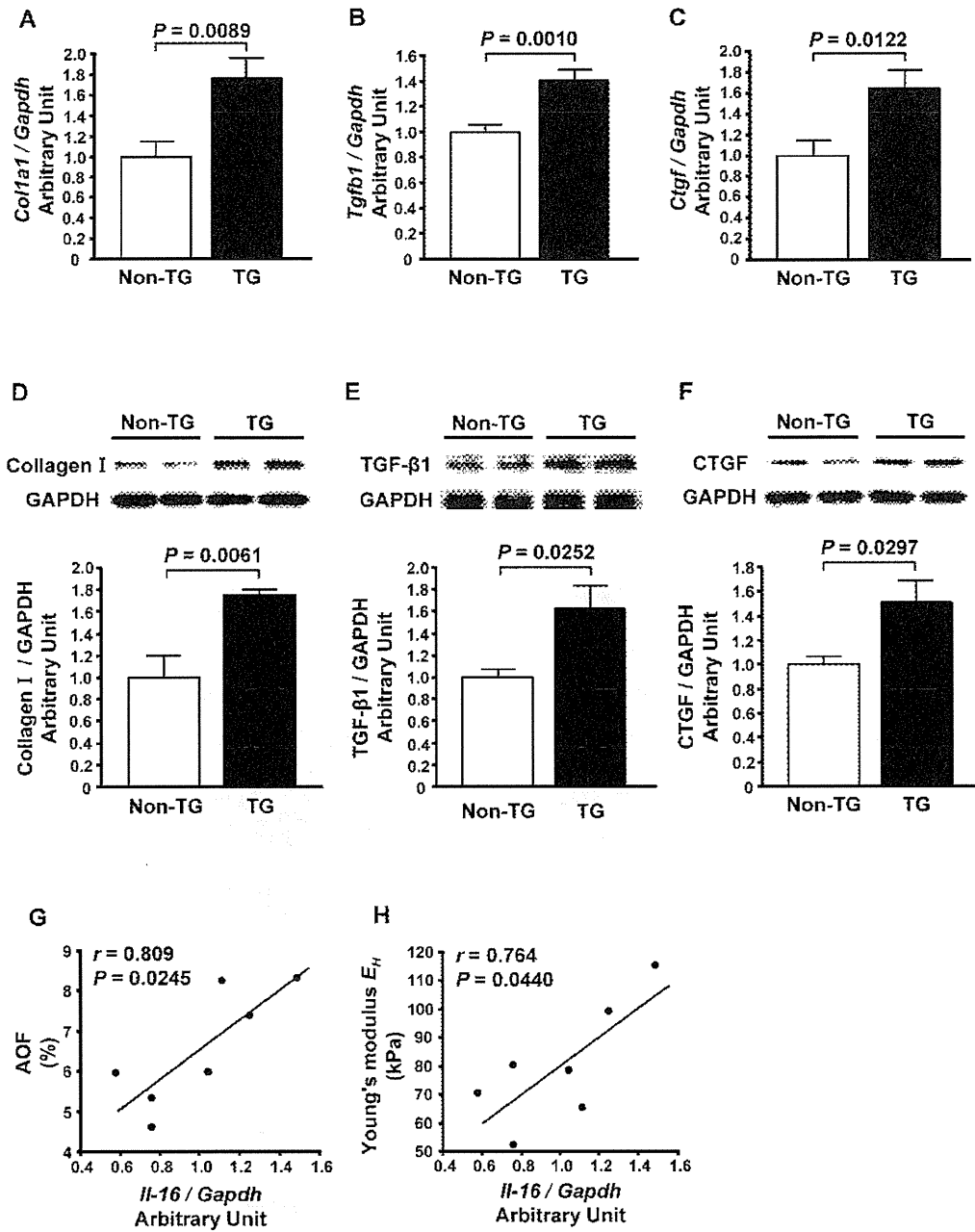


**Figure 4. Effect of enhanced cardiac expression of interleukin-16 (IL-16) on markers of cardiac fibrosis in mice.** A through C, Left ventricular mRNA levels of Collagen I (A), transforming growth factor-beta 1 (TGF-β1) (B) and connective tissue growth factor (CTGF) (C) in non-transgenic (Non-TG) and transgenic (TG) mice. D through F, Left ventricular protein levels of Collagen I (D), TGF-β1 (E) and CTGF (F) in Non-TG and TG mice. Top panels in each figure show a representative Western blot. *n* = 5 per group. G and H, Correlations of IL-16 mRNA levels with AOF (G) and Young's modulus  $E_H$  (H) in TG mice. doi:10.1371/journal.pone.0068893.g004

**Table 5.** Comparison of anatomical and functional characteristics of the TG and Non-TG mice.

	Non-TG (n=8)	TG (n=7)
Body weight, g	36.8±1.2	37.5±1.2
Systolic blood pressure, mmHg	93±2	97±2
Heart rate, bpm	633±22	625±13
LV weight/body weight, mg/g	3.40±0.17	2.95±0.11
Atrial weight/body weight, mg/g	0.25±0.01	0.39±0.05*
Lung weight/body weight, mg/g	4.12±0.25	4.27±0.13
<b>Echocardiography</b>		
LV end-diastolic dimension, mm	3.76±0.10	3.84±0.11
PWd, mm	0.98±0.03	0.95±0.04
Fractional shortening, %	41±2	43±1

Data are mean ± SEM. LV indicates left ventricular; and PWd, LV posterior wall thickness at end-diastole.

\* $P < 0.05$  vs. Non-TG mice.

doi:10.1371/journal.pone.0068893.t005

## Results

### Serum IL-16 Levels are Elevated in HFpEF Patients and Associated with LV Diastolic Dysfunction

First, we analyzed serum samples from the HFpEF and HFrEF patients and controls (Table 1) using a multiplex-bead array assay for screening the 50 cytokines, chemokines, growth factors, angiogenic factors and soluble receptors. This analysis revealed that serum IL-16 levels were significantly higher in patients with HFpEF than in patients with HFrEF or in controls (Figure 1A). Although we also found significant differences in several analytes other than IL-16 among the three groups (Table 2), we decided to focus on IL-16 because of the specific increase of IL-16 in HFpEF patients.

Next, we included more HFpEF patients and controls, and measured the serum IL-16 levels by ELISA to confirm the results obtained by the multiplex-bead array assay. The characteristics of the total study patients are shown in Table 3. LV ejection fraction was not significantly different between the two groups, whereas LV end-systolic and diastolic dimensions were significantly larger in the HFpEF group than in the control group, which is consistent with previous reports [36]. Analysis of serum levels of IL-16 in this larger population confirmed that IL-16 was significantly higher in HFpEF patients than in controls (Figure 1B). Moreover, serum

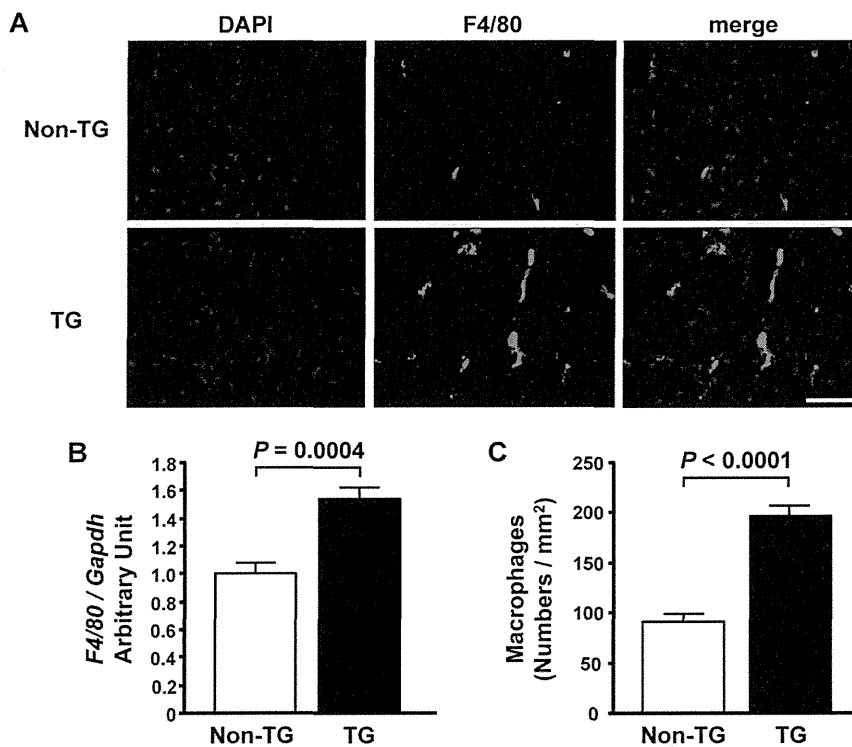


**Figure 5. Enhanced cardiac expression of interleukin-16 induces cardiac macrophage infiltration in mice.** A, Representative photomicrographs of immunofluorescence staining of the left ventricle for F4/80 in non-transgenic (Non-TG) and transgenic (TG) mice. Bar = 50  $\mu$ m. B, Left ventricular mRNA levels of F4/80 in Non-TG and TG mice. C, Quantitative analysis of macrophage infiltration into left ventricular myocardium in Non-TG and TG mice.  $n = 6$  per group. doi:10.1371/journal.pone.0068893.g005

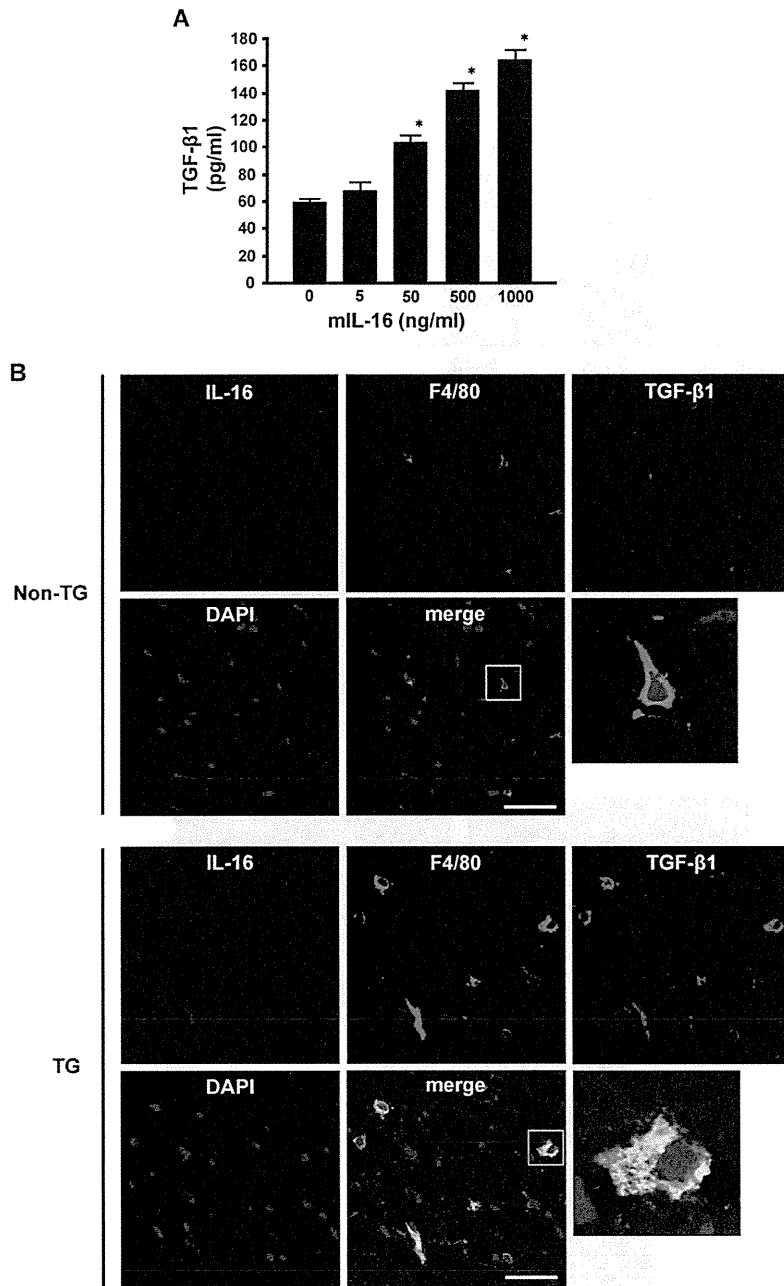


**Figure 6. Effect of interleukin-16 (IL-16) on transforming growth factor-beta 1 (TGF-β1) production by macrophages.** **A**, Production of TGF-β1 by macrophages treated with murine recombinant IL-16 (mIL-16). Mouse peritoneal macrophages ( $2 \times 10^6$  cells/well) were treated with the indicated concentration of mIL-16 for 24 hours. The supernatants of macrophage cultures were collected and TGF-β1 was measured as described in the Methods.  $n = 5$  for each group.  $*P < 0.05$  vs. 0 ng/ml group. **B**, Representative photomicrographs of confocal immunofluorescence staining of the left ventricle in non-transgenic (Non-TG) and transgenic (TG) mice for IL16 (violet), F4/80 (green), and TGF-β1 (red). doi:10.1371/journal.pone.0068893.g006

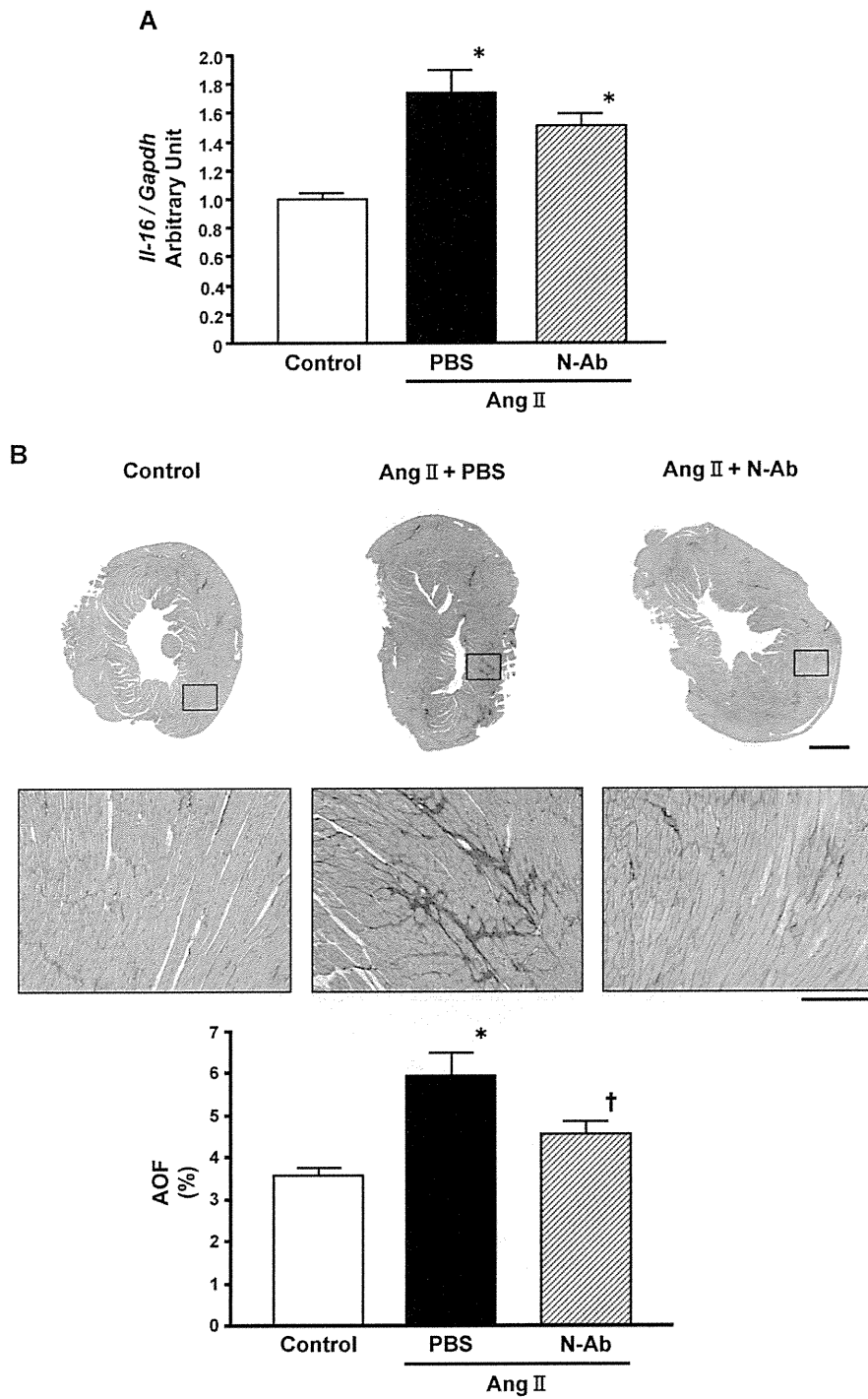


**Figure 7. Neutralization of interleukin-16 (IL-16) ameliorates the development of cardiac fibrosis.** **A**, mRNA level of IL-16 in the left ventricle of control mice and mice injected intraperitoneally with phosphate buffered saline (PBS) or anti-IL-16 neutralizing antibody (N-Ab) during angiotensin II (Ang II) infusion for 14 days. \* $P < 0.05$  vs. control group. **B**, Representative photomicrograph of Sirius Red-stained heart sections and the percent area of fibrosis (AOF) in control mice and mice injected intraperitoneally with PBS or N-Ab during Ang II infusion for 28 days. Bar: Upper panel = 1 mm; Lower panel = 200  $\mu$ m. \* $P < 0.05$  vs. control group. † $P < 0.05$  vs. mice with PBS treatment during Ang II infusion. doi:10.1371/journal.pone.0068893.g007

levels of IL-16 were positively correlated with the  $E/e'$  ratio and LAVI when both groups were combined (Figure 1C and D). These results suggested a possible association between IL-16 and indices of LV diastolic dysfunction and/or elevation of LV filling pressure in human subjects. In addition, we observed a correlation between serum IL-16 levels and DWS, suggesting that elevation of IL-16 is associated with LV stiffening in human subjects (Figure 1E).

#### Serum IL-16 Levels and Cardiac Expression of IL-16 are Elevated in the HFpEF Rats

To examine whether the elevation in serum IL-16 and its association with diastolic dysfunction is a common phenomenon in HFpEF, we analyzed a rat model of HFpEF. The changes in myocardial anatomy and function induced by hypertension in our HFpEF model (Table 4) were similar to changes that have been described in previous reports [6,7,17,23,27].

The serum levels of IL-16 were significantly higher in rats with HFpEF than in control rats (Figure 2A), and positively correlated with LVEDP and the ratio of lung weight to body weight in all rats (Figure 2B and C). Although there was no correlation between serum IL-16 levels and Tau ( $r = 0.331$ ,  $P = 0.1561$ ), we found a positive correlation between serum IL-16 levels and MSC (Figure 2D), suggesting that elevation of IL-16 in HFpEF rats is associated with LV myocardial stiffening but not with LV abnormal relaxation. Furthermore, expression of IL-16 mRNA in the left ventricle was higher in HFpEF rats than in control rats (Figure 2E).

#### Enhanced Cardiac Expression of IL-16 causes Myocardial Fibrosis and Stiffness

To assess the effect of enhanced cardiac expression of IL-16, we generated TG mice carrying murine IL-16 cDNA under the control of the  $\alpha$ -MHC promoter. We identified four transgene positive founders by PCR. Among them, germline transmission

was observed in three lines (line 13, 21, and 22). The line 21 mice expressing the highest myocardial levels of the transgene were bred and analyzed.

The enhanced expression of the bioactive secreted form of IL-16 in the heart of TG mice was confirmed by Western blotting (Figure 3A), whereas there was no significant difference in serum IL-16 levels between TG ( $32.1 \pm 6.8$  pg/ml) and Non-TG ( $31.3 \pm 6.0$  pg/ml) mice. Atrial enlargement was observed (Table 5 and Figure 3B) and the extent of LV fibrosis was increased (Figure 3C) in the TG mice. Moreover, an index of LV myocardial stiffness, Young's modulus  $E_H$ , was also increased in the TG mice (Figure 3D). LV mRNA and protein levels of Collagen I, TGF- $\beta$ 1 and CTGF were also increased in the TG mice (Figure 4A through F). The LV IL-16 mRNA level was positively correlated with both the extent of LV fibrosis and  $E_H$  in the TG mice (Figure 4G and H).

#### Macrophages are Involved in Cardiac Fibrosis Caused by Enhanced Cardiac Expression of IL-16

Inflammatory cells, especially infiltrating monocytes and macrophages in the heart, have been suggested to have a crucial role in cardiac fibrosis [17,37,38], whereas IL-16 has been reported to be able to chemoattract monocytes [39]. Therefore, we examined macrophage infiltration into LV myocardium of TG mice and assessed the direct effect of IL-16 on cultured macrophages. Macrophages were significantly increased in the left ventricle of TG mice (Figure 5A through C). In addition, when stimulated with recombinant murine IL-16, mouse peritoneal macrophages released TGF- $\beta$ 1 in a dose-dependent manner (Figure 6A). Confocal immunofluorescence microscopy revealed that many F4/80-positive macrophages colocalized with TGF- $\beta$ 1 in the left ventricle of TG mice compared with Non-TG mice (Figure 6B). These data suggested that IL-16 might be at least one of the cytokines playing a central role in the promotion of cardiac fibrosis through the release of TGF- $\beta$ 1 from the infiltrating and resident macrophages in TG mice.

**Table 6.** Comparison of control mice and angiotensin II-infused mice treated with PBS or anti-IL-16 neutralizing antibody.

	Control (n=12)	Ang II+PBS (n=12)	Ang II+N-Ab (n=11)
Body weight, g	27.2±0.3	25.2±0.3*	25.1±0.3*
Systolic blood pressure, mmHg	102±1	152±5*	159±5*
Heart rate, bpm	679±7	678±13	665±9
LV weight/body weight, mg/g	3.49±0.06	4.87±0.14*	4.67±0.19*
Atrial weight/body weight, mg/g	0.25±0.01	0.38±0.02*	0.33±0.01*†
Lung weight/body weight, mg/g	4.86±0.05	5.61±0.09*	5.38±0.04*†
<b>Echocardiography</b>			
LV end-diastolic dimension, mm	3.75±0.06	3.26±0.04*	3.20±0.06*
PWd, mm	0.82±0.01	1.10±0.02*	1.10±0.04*
Fractional shortening, %	44±1	42±1	45±2

Data are mean ± SEM. Ang indicates angiotensin; LV, left ventricular; N-Ab, anti-IL-16 neutralizing antibody; PBS, phosphate buffered saline; and PWd, LV posterior wall thickness at end-diastole.

\* $P < 0.05$  vs. control group.

† $P < 0.05$  vs. Ang II+PBS group.

doi:10.1371/journal.pone.0068893.t006